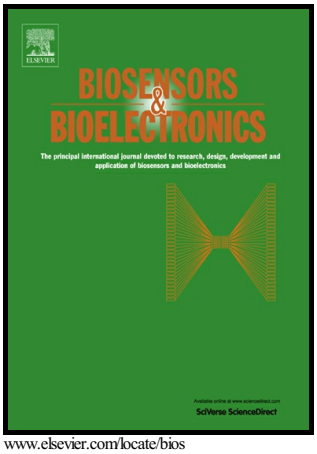

www.elsevier.com/locate/bios

Immobilized-free miniaturized electrochemical sensing system for Pb^{2+} detection based on dual Pb^{2+}-DNAzyme assistant feedback amplification strategy

Wei Cai, Shunbi Xie, Jin Zhang, Dianyong Tang, Ying Tang

PII: S0956-5663(18)30451-2
DOI: https://doi.org/10.1016/j.bios.2018.06.020
Reference: BIOS10540

To appear in: *Biosensors and Bioelectronic*

Received date: 6 March 2018
Revised date: 31 May 2018
Accepted date: 7 June 2018

Cite this article as: Wei Cai, Shunbi Xie, Jin Zhang, Dianyong Tang and Ying Tang, Immobilized-free miniaturized electrochemical sensing system for Pb^{2+} detection based on dual Pb^{2+}-DNAzyme assistant feedback amplification strategy, *Biosensors and Bioelectronic,* https://doi.org/10.1016/j.bios.2018.06.020

Immobilized-free miniaturized electrochemical sensing system for Pb^{2+} detection based on dual Pb^{2+}-DNAzyme assistant feedback amplification strategy

Wei Cai[a,b], Shunbi Xie[a*], Jin Zhang[a,b], Dianyong Tang[a], Ying Tang[a*]

[a] *Chongqing Key Laboratory of Environmental Materials and Remediation Technologies (Chongqing University of Arts and Sciences), Chongqing University of Arts and Sciences, Chongqing 402160, PR China*

[b] *Key Laboratory of Luminescent and Real-Time Analytical Chemistry (Southwest University), Ministry of Education, College of Chemistry and Chemical Engineering, Southwest University, Chongqing 400715, PR China*

Abstract

We presented a novel dual-DNAzyme feedback amplification (DDFA) strategy for Pb^{2+} detection based on a micropipette tip-based miniaturized homogeneous electrochemical device. The DDFA system involves two rolling circle amplification (RCA) processes in which two circular DNA templates (C1 and C2) have been designed with a Pb^{2+}-DNAzyme sequence (8-17 DNAzyme, anti-GR-5 DNAzyme) and an antisense sequence of G-quadruplex. And a linear DNA (L-DNA), which

*Corresponding authors. Tel.: +86-23-61162815.

E-mail address: tangying2282@163.com (Y. Tang); xieshunbi@163.com (S. B. Xie)

consists of a primer sequence and a Pb^{2+}-DNAzyme substrate sequence, could hybridize with C1 and C2 to form two DNA complexes. In presence of Pb^{2+}, the Pb^{2+}-DNAzyme exhibited excellent cleavage specificity toward the substrate sequence in L-DNA, leaving primer sequence to trigger two paths of RCA process and finally resulting in massive long nanosolo DNA strands with reduplicated G-quadruplex sequences. And then, methylene blue (MB) could selectively intercalate into G-quadruplex to reduce the free MB concentration in the solution. Thereafter, a carbon fiber microelectrode-based miniaturized electrochemical device was constructed to record the decrease of electrochemical signal due to the much lower diffusion rate of MB/G-quadruplex complex than that of free MB. Therefore, the concentration of Pb^{2+} could be correctively and sensitively determined in a homogeneous solution by combining DDFA with miniaturized electrochemical device. This protocol not only exhibited high selectivity and sensitivity toward Pb^{2+} with a detection limit of 0.048 pM, but also reduced sample volume to 10 μL. In addition, this sensing system has been successfully applied to Pb^{2+} detection in Yangtze River with desirable quantitative manners, which matched well with the atomic absorption spectrometry (AAS).

Keywords: feedback amplification strategy, homogeneous electrochemical biosensor, carbon fiber microelectrode, rolling circle amplification, Pb^{2+}-DNAzyme

1. Introduction

Lead ion (Pb^{2+}), which is one of the most toxic and wildly distributed heavy metal ions in the environment, has caused significant concerns of the scientific

community (Sun et al., 2018; Cai et al., 2017; Rudd et al., 2016). In the past years, the detection of Pb^{2+} was mainly dependent on instrument analysis such as mass spectrometry, spectrometry and inductive coupled plasma (ICP), but the inherent shortcomings (e.g., complicated pretreatment, bulky apparatus and expensive testing costs) limited their application to the laboratory (Zhou et al., 2016; Li et al., 2017). Therefore, the development of high sensitive and low-cost technologies for routine monitoring of Pb^{2+} hold great significance (Liang et al., 2017; Zang et al., 2014). Electrochemical methods with distinct virtues of low-cost, simple instrumentation and excellent analytical performance, have achieved great progress in the past few years (Yu et al., 2018; Shin et al., 2017). Nevertheless, most of current existing electrochemical biosensors still suffer from redundant immobilization procedures, tedious clean steps and non-renewable electrode surface (Shin et al., 2017; Hou et al., 2015; Tan et al., 2016). To overcome these disadvantages, researchers focus their attention on the development of immobilized-free and reusable miniaturization electrochemical biosensors for applying to complex biological and environmental samples.

With the breakthrough of microfabrication and printing technologies, miniaturized electrochemical biosensors have became increasingly popular in the area of point-of-care testing (Sempionatto et al., 2017; Hrdy et al., 2017; Hsieh et al., 2012), environmental protection (Huang et al., 2017; Chalupniak et al., 2017; Zhao et al., 2017), as well as biological analysis (Liu et al., 2017a; Zhang et al., 2017a, 2017b; Xu et al., 2018). Among them, carbon fiber microelectrode (CFME) attracts

considerable interests in biomedical detection and environmental monitoring due to its virtue of inexpensive, biocompatibility, high mechanical strength and easy miniaturization. Although CFME exhibits excellent analytical performance and obvious advantages than typical bulk electrode, the small size also poses great difficulty for its manufacturing. Ohsaka's group reported a third-generation biosensor for superoxide anion detection based on a CFME (Tian et al., 2005). In this method, the CFME is sealed by epoxy resin at 100 ℃ for 2 h, the harsh seal conditions inevitably lead to poor sealing and increase the difficulty in the fabrication process. Subsequently, Cheng's group have developed a facile method to fabricate a low-noise CFME by using flame-fuse seal procedure to replace the traditional epoxy sealing, achieving effective insulation without any pollution (Huang et al., 2001). However, it is difficult to guarantee the carbon fiber survival from the flame of gas lamp in sealing process. Recently, Huang's group has provided a facile way to solve this problem by using wax to seal the SiC nanowire in glass pipette (Zhang et al., 2017). While the good electrical contact of the SiC nanowire is achieved by filling liquid metal in glass pipette which inevitably cause unnecessary heavy metal pollution. In this context, we constructed a facile, high production and environmentally friendly CFME that covered the aforementioned drawbacks and successfully demonstrated its application to Pb^{2+} detection in river water samples.

At present, Pb^{2+}-dependent DNAzyme-based methodologies have gradually emerged as dominant sensing strategies for Pb^{2+} detection because of their versatility and high catalytic activity and good compatibility (Li et al., 2010; Shi et al., 2016).

These fascinating virtues make them easily integrate with various kinds of DNA amplification techniques, such as polymerase chain reaction (PCR) (Wang et al., 2010; Zhu et al., 2015), hybridization chain reaction (HCR) (Zhuang et al., 2013) and rolling circle amplification (RCA) (Kim et al., 2016; Tang et al., 2013). As far as we know, there are two types of DNAzyme, GR-5 DNAzyme and 8-17 DNAzyme, have been extensively used to develop Pb^{2+} specific recognition biosensors. Interestingly, we found that 8-17 DNAzyme and GR-5 DNAzyme could recognize the same substrate at the same conditions (Zhao et al., 2011; Elbaz et al., 2008). Therefore, we speculated that if we could integrate the two categories of Pb^{2+}-DNAzymes into one amplification system to develop a novel signal amplification strategy for high sensitivity detection of Pb^{2+}. Recently, Li's group reported a feedback amplification strategy that incorporates DNAzyme into RCA process to create a feedback circuit for DNA amplification sensing (Liu et al., 2017b). Inspire by the feedback design, we attempt to incorporate 8-17 DNAzyme and GR-5 DNAzyme into RCA process to create a novel feedback strategy, which could obviously enhance the sensitivity than the method that only has one Pb^{2+}-DNAzyme.

In this work, we integrated dual Pb^{2+}-DNAzyme into RCA process to create a novel feedback amplification strategy and demonstrated its high potential for amplifying Pb^{2+} sensing in river water samples. The use of dual Pb^{2+}-DNAzyme as recognition elements for triggering RCA process endow this amplification technology with excellent selectivity and sensitivity toward Pb^{2+}. Furthermore, we also presented an extremely facile yet efficient method for fabricating CFME by using wax as a

unique sealant to replace traditional epoxy-seal or flame-fuse methods, which make the fabrication process more simple and robust. As the dimension of CFME perfectly matched with commercial micropipette tip (10 μL), it allow us to develop a miniaturized electrochemical device to achieve sample volume down to 10 μL. Therefore, combining with the proposed DDFA strategy with the CFME-based miniaturized electrochemical device, this sensing system may hold a promising prospect for Pb^{2+} detection in real samples at the microliter level.

2. Experiment section

2.1 Procedures of the DDFA

Phosphorylated circular DNA template C1 (100 nM), C2 (100 nM) and L-DNA (200 nM) was mixed in 40 μL H_2O. Then, the mixture was denatured at 90 °C for 5 min, followed slowly cooled down to room temperature. After that, 5 μL of 10 × T4 DNA ligase buffer (400 mM Tris-HCl, 100 mM $MgCl_2$, 100 mM DTT, 5 mM ATP, pH 7.8) and 1 μL T4 DNA ligase (5 U) was added and watered total volume to 50 μL. The obtained mixture was incubated at 4 °C for overnight to ensure the formation of DNA complexes L-DNA/Cir1 and L-DNA/Cir2. Then, the ligase reaction was terminated by heating for 10 min at 65 °C. The DDFA was conducted in 80 μL solution that containing 50 μL above-prepared ligation products, 8 μL of 10 × phi 29 buffer (330 mM tris-acetate (pH 7.9 at 37 °C), 100 mM Mg-acetate, 660 mM K-acetate, 1% (*v*/*v*) tween 20, 10 mM DTT), 1.6 μL of phi 29 DNA polymerase (phi 29, 10 U/μL), 1.6 μL of T4 polynucleotide kinase (PNK, 10 U/μL), 3.2 μL of dNTP

mixture solution (25 mM each of dATP, dCTP, dGTP, dTTP) and 10 μL different concentrations of Pb^{2+}. After incubating for 120 min at 37 °C, the feedback amplification reaction was terminated by heating for 10 min at 65 °C.

2.2 Electrochemical assay for Pb^{2+}

Prior to monitor, the CFME was dipped in water for washing three times. Then, 2 μL of MB solution (80 μM) was added into 80 μL of the above obtained DDFA solution and incubated for 18 min at 37 °C to form stable G-quadruplex/MB complexes, which was employed as the following analyte solution. Subsequently, the as-prepared CFME was tightly inserted into a micropipette tip which correctly aspirated with 10 μL analyte solution. After that, the miniaturized electrochemical device was placed in an electrochemical cell for further detection.

2.3 Gel electrophoresis analysis

The feasibility of DDFA was analyzed by 10% non-denaturation polyacrylamide gel (PAGE) and 10% denaturing urea polyacrylamide gel electrophoresis (Urea-PAGE), respectively. In the gel electrophoresis, analyte samples were loaded into the notches of freshly prepared gel and run at 120 V for 60 min in 1 × TBE buffer, and then stained with 4S Green for 40 min. Finally, the gel was imaged by Tanon 5200 Multi Chemiluminescent/Fluorescence Image System.

2.4 Colorimetric Characterization

100 μL 1× RCA buffer solution that contained different RCA amplification products and 2 μM hemin were prepared for colorimetric assay. After incubating for

40 min at room temperature, 2 μL of ABTS (20 mM, final concetration), 1 μL of H_2O_2 (8.8 mM, final concetration) were added, and then the resultant samples were imaged immediately with a digital camera.

2.5 Samples Preparation

River water samples were obtained from Yangtze River (Chongqing, China) and acidulated by 37% HCl (100:1 *v*/*v*). Then, the river samples were filtered through a 0.45 μm membrane to remove larger insoluble particles and algae. Thereafter, 10 μL of water samples was spiked into the ligase product to trigger the feedback amplification process, and the detection procedures were the same as above mentioned. The real concentrations of Pb^{2+} in river samples were monitored by AAS.

3. Results and discussion

3.1 Design and detection principle

The design and sensing principle of the DDFA is illustrated in Scheme 1. In this system, two circular DNA templates (C1 and C2) and linear DNA (L-DNA) have been subtly designed: (I) C1 consists of a sequence of 8-17 DNAzyme and an antisense sequence of G-quadruplex (anti-G-quadruplex), (II) C2 contains an antisense sequence of GR-5 DNAzyme (anti-GR-5 DNAzyme) and the same sequence of anti-G-quadruplex, and (III) L-DNA comprises of three parts, a linear oligonucleotide sequence for hybridizing with C1 or C2, a RNA-containing sequence for acting as Pb^{2+}-DNAzyme substrate, and 3'-ends labeled inverted dT (invdT) for inhibiting the extension of phi 29 (Bryda et al., 2006). Both C1 and C2 could

hybridize with L-DNA to form two DNA hybridization complexes L-DNA/Cir1 and L-DNA/Cir2 with the assistance of T4 DNA ligase. In the absence of Pb^{2+}, 8-17 DNAzyme lacks any biocatalytic activity and no cleavage reaction towards L-DNA. As a result, the majority of MB molecules in the solution are present at a free state, exhibiting good diffusivity toward the CFME surface, and thus leading to a large diffusion current. On the contrary, in the presence of Pb^{2+}, the cleavage activity of 8-17 DNAzyme is activated, which could specifically cleave the L-DNA at the RNA-marked cleave site, the leaving fragment which hybridize with Cir2 is served as a primer for the following RCA amplification step. After treated the primer with PNK to remove the 2,3-cyclic phosphate (Zhao et al., 2013; Brown et al., 2003), the C2-mediated RCA process could be performed in the presence of phi 29 and dNTPs, producing a long nanosolo DNA with massive repeated G-quadruplex sequences and GR-5 DNAzyme units. The generated GR-5 DNAzyme units could be further hybridized with L-DNA in L-DNA/Cir1 complex to trigger another C1-mediated RCA process, yielding more nanosolo DNA with repeated G-quadruplex sequences. Therefore, a large number of G-quadruplex sequences would be synthesized in the solution after the feedback RCA amplification process. And the obtained massive G-quadruplex could capture the free MB in the solution due to the strong affinity between MB and G-quadruplex, inhibiting the diffusion of MB toward CFME surface and finally resulting in a weak diffusion current (Zhang et al., 2014; Liu et al., 2017c). With such design, the concentration of Pb^{2+} could be correctly determined with high sensitive based on the prepared miniaturized electrochemical sensing system.

(Scheme 1)

3.2 Characterization of the CFME

The preparation process of carbon fiber microelectrode was illustrated in Figure S-1B. The morphology of the wax-sealed microelectrode was characterized by SEM and invert fluorescence microscope. The SEM image of the interface of carbon fiber and wax was shown in Figure 1A. We could clearly see that the carbon fiber was well sealed into a glass capillary with a diameter of 7.303 μm (Figure 1B). The increasing diameter of the carbon fiber was attributed to the coated Au-layer, which was used to facilitate the microscopic visualization in SEM analysis. To obtain a deeper insight, we also provided the fluorescence microscope images. As displayed in Figure 1C, the carbon fiber was tightly sealed into the tip of glass capillary by waxing with a protruding length approximately 2 mm. In addition, a close-up microscope image of the joint of copper wire and carbon fiber was displayed in Figure 1D. The carbon fiber was well-connected with copper wire which insures the good electrical connection of CFME.

(Figure 1)

As the electron transfer of $Fe(CN)_6^{3-/4-}$ could directly reflect the nature of electrode surface, cyclic voltammetric (CV) in 5 mM $Fe(CN)_6^{3-/4-}$ was employed to evaluate the electrochemical performance of CFME. First of all, we studied the feasibility of the CFME-based miniaturized electrochemical device (Figure S-2). From the almost identical quasi-steady state current of the CFME in the bulky

electrochemical cell and micropipette tip, we could figure out that the fabrication of the micropipette tip-based electrochemical device using wax-sealed CFME was successful and feasible. The CV behaviors of CFME with various scan rates from 20 to 300 mV/s in 5 mM $Fe(CN)_6^{3-/4-}$ was explored in Figure S-3A. The peak currents of cathodic and anodic increase linearly with the square root of scan rate (Figure S-3B), suggesting a diffusion controlled process of the electron reaction. Furthermore, the stability of the electrochemical device was verified by consecutive steady-state cyclic voltammograms in 5 mM $Fe(CN)_6^{3-/4-}$ at scan rate of 0.1 V/s. As shown in Figure S-4A, just 1.38% and 5.14% of the oxidation and reduction currents decrement were found after consecutive scanning 100 cycles, indicating the analyte solution leaking from the micropipette tip to the electrochemical cell could be almost negligible within 1 min electrochemical detection time. In other words, the electrochemical device based on wax-sealed microelectrode could maintain good stability even at a small sample solution down to 10 μL. Meanwhile, the reusability of the CFME was also investigated by repeated monitoring 10 μL analyte samples for 10 times with ACV measurement. As shown in Figure S-4B, when the CFME was used to measure in the analyte samples, obvious signal responses could be observed (defined as n′, n = 1, 2 …), while no electrochemical response was appeared when the CFME was measured the 0.1 M PBS solution (defined as n, n = 1, 2 …). This behavior implied that the wax-sealed CFME was not contaminated during the Pb^{2+} detection and could be reused for many times. The aforementioned evidences informed that the wax-sealed CFME and electrochemical device were successfully prepared with

excellent electrochemical properties.

3.3 Feasibility of the DDFA

The catalytic activity of dual Pb^{2+}-DNAzyme was a prerequisite for successful implementation of DDFA. Thus, the cleavage activity of the dual Pb^{2+}-DNAzyme was firstly validated by 10% denaturing Urea-PAGE (see Figure S-5 and Figure S-6 in supporting information). In order to investigate the DNA configuration and the feasibility of the DDFA for Pb^{2+} sensing, a 10% non-denaturation PAGE was employed to analyze the reaction process. As shown in Figure 2A, bands corresponding to C1, C2 and L-DNA could be obviously observed in lanes 2-4, respectively. When the mixture of C1 and L-DNA and the mixture of C2 and L-DNA were incubated with T4 ligase, two bands with higher molecular-weight separately appeared in lane 5 and lane 6, demonstrating the L-DNA/Cir1 and L-DNA/Cir2 were successfully prepared. Finally, when the reaction of the feedback amplification sensing system was incubated with Pb^{2+}, an obvious higher molecular-weight band was presented in lane 8. In contrast, there was no new band appeared when the feedback amplification system was absence of Pb^{2+} (lane 9), which was matched well with the bands of the ligase product of C1, C2 and L-DNA (lane 7). This behavior proved that the design of oligonucleotides in the sensing system was reasonable for determination of Pb^{2+}.

(Figure 2)

3.4 Contribution of DDFA for signal amplification

In this study, DDFA was designed as an effective method for target amplification sensing. For evaluating and demonstrating the contribution of the feedback amplification strategy, the sensing system without and with C2-mediated RCA process was investigated by ACV. As seen from Figure 2B, when the sensing system was just amplified with C1-mediated RCA process (b), an obvious electrochemical signal reduction (ΔI = 21 nA) was founded comparing with the blank sample (a). While when the amplification sensing system was mediated by dual Pb^{2+}-DNAzyme with two RCA amplifications (c), the diffusion current of MB was significantly decreased (ΔI = 39 nA), demonstrating that feedback-based two RCA amplification system could effectively enhance the change of electrochemical signal. Besides, the colorimetric characterization was further adopted to identify the above conclusion. Hemin could incorporate into G-quadruplex to form a horseradish peroxidase-mimicking DNAzyme (hemin/G-quadruplex), which could catalyze oxidization chromogenic substrate ABTS [2,2'-azino-bis(3-ethylbenzothiazoline-6-sulfonate)] to induce a color change and produce a absorption spectra of $ABTS^{\bullet+}$ in the presence of hydrogen peroxide. As shown in Figure 2C, when the feedback amplification system was absence of Pb^{2+}, the color of the solution has hardly changed and generated a weak absorbance signal (a), because there was no hemin/G-quadruplex formation. In contrast, when the amplification system was mediated by the dual Pb^{2+}-DNAzyme assistant feedback RCA process, the color of the solution changed from colorless to deep green, and produced an obvious increase of the absorbance signal (c). However, the response of the amplification system that

just amplified with C1-mediated RCA process (b) was much lower than that mediated by the dual Pb^{2+}-DNAzyme assistant feedback RCA process. This phenomenon was ascribed to the fact that dual Pb^{2+}-DNAzyme triggered RCA process could produce more G-quadruplex sequences production, resulting in higher peroxidase-like catalytic activity.

3.5 Quantitative detection of Pb^{2+}

Under the optimized conditions (Figure S-7), a serial of concentrations of Pb^{2+} were utilized to evaluate the analytical performance of this sensing system. As shown in Figure 3A, the diffusion current of MB was continuously reduced with the concentration of Pb^{2+} increasing from 0 to 100 nM, which suggested that higher concentration of Pb^{2+} could induce more G-quadruplex production, thereby generating a lower diffusion current. A good linear correlation between ACV peak current and the logarithm concentration of Pb^{2+} range from 0.2 pM to 100 nM was presented in Figure 3B. The correlation equation was determined to be I = -9.95 lg$c$ (nM) + 298.97, with a correlation coefficient of r = 0.9985. The limit of detection was measured to be 0.048 pM (evaluated at a signal-to-noise of 3σ, where σ is the standard deviation of a blank solution, n = 11), which obviously lower than the definition of EPA (The United States Environmental Protection Agency) for Pb^{2+} detection in drinking water (72.4 nM) (Shi et al., 2016). In addition, compared with the previous reported free-immobilized and immobilized-based electrochemical assays (Table S-2), our prepared sensing system showed a lower limit of detection and wider linear range.

The higher sensitivity of this sensing system was mainly attributed to significant amplification of the feedback RCA amplification strategy.

(Figure 3)

3.6 Selectivity of the proposed sensing system

The selectivity of this homogeneous sensing system was evaluated by adding a series of metal irons commonly coexisting with Pb^{2+} in the environment, such as Fe^{3+}, Mn^{2+}, Ag^{+}, Ba^{2+}, Cu^{2+}, Al^{3+}, Ca^{2+}, Ni^{2+}, Cd^{2+}, Co^{2+}, Cr^{3+} and Hg^{2+}. As shown in Figure 4A, a notable current decrease could be observed when the system was incubated with 0.5 nM Pb^{2+}, whereas no obvious changes were found for the interference metal ions, even with high concentrations (50 nM). This result suggested that our prepared sensing system possesses of excellent selectivity for Pb^{2+} detection, which mainly attributed to the high selectivity of 8-17 DNAzyme and GR-5 DNAzyme to Pb^{2+}. To further investigate the reproducibility of the proposed sensing system, we evaluated the ACV responses of five different CFME-based electrochemical devices that made in the same batch. As seen from Figure 4B, the relative standard deviations (RSD) was 1.22%, indicating the reproducibility and precision of the developed sensing system were acceptable.

(Figure 4)

3.7 Application in real samples

To investigate the analytical reliability of the proposed sensing system in

practical applications, it was applied to detect the free Pb^{2+} in river water samples, which obtained from Yangtze River (Chongqing, China). The analytical results were displayed in Table 1, we could clearly see that the recovery values ranging from 94.7% to 106.7% with a satisfactory RSD, which matched well with the AAS analytical data. This result indicated that this sensing system we prepared provided a bright prospect in Pb^{2+} detection in environmental samples.

(Table 1)

4. Conclusions

In summary, we have designed a novel feedback amplification strategy for highly sensitive detection of Pb^{2+} based on a dual Pb^{2+}-DNAzyme assistant RCA process and an immobilized-free homogeneous miniaturized electrochemical device. Using DNAzyme as the recognition element to trigger two categories of RCA process ensures the excellent selectivity of the sensing system. As Pb^{2+} was able to induce two paths of RCA process to create feedback amplification, a small amount of target Pb^{2+} could generate abundant of G-quadruplex sequences to induce a strong electrochemical signal reduction, thus achieving a highly sensitive sensing system. Furthermore, a facile and efficient method was presented for CFME fabrication by using wax as the sealant to seal carbon fiber into glass capillary. The wax-sealed CFME could achieve a controllable protruding length of carbon fiber with stable and effective insulation. Besides, using the wax-sealed CFME to fabricate miniaturized electrochemical device for Pb^{2+} detection not only exhibited good analytical

performance, but also reduced the sample solution to several microliters. In addition, the resultant sensing system can be applied to river water samples with desirable quantitative manners, which provides a promising perspective for routine testing.

Acknowledgements

This work was financially supported by the National Natural Science Foundation of China (21705013), the Chongqing Science and Technology Commission of China (cstc2017jcyjAX0282, cstc2015jcyjBX0126, cstc2016shmsZX20001), the Science and Technology Research Program of Chongqing Municipal Education Commission China (KJ1711265, KJ1711285), the Foundation for High-level Talents of Chongqing University of Arts and Sciences, China (R2016CH08), Chongqing Yongchuan District Water Authority (2016-07).

Notes

The authors declare no competing financial interest.

References

Brown, A. K., Li, J., Pavot, C. M. B., Lu, Y., 2003. Biochemistry 42, 7152-7161.

Bryda, E. C., Pearson, M., Agca, Y., Bauer, B. A., 2006. Biotechniques 41, 715-719.

Cai, F. X., Wang, Q. H., Chen, X. Q., Qiu, W. W., Zhan, F. P., Gao, F., Wang, Q. X., 2017. Biosens. Bioelectron. 98, 310-316.

Chalupniak, A, Merkoci, A., 2017. ACS Appl. Mater. Interfaces 9, 44766-44775.

Elbaz, J., Shlyahovsky, B., Willner, I., 2008. Chem. Commun. 1569-1571.

Hou, T., Li, W., Liu, X. J., Li, F., 2015. Anal. Chem. 87, 11368-11374.

Hrdy, R., Kynclova, H., Klepacova, I., Bartosik, M., Neuzil, P., 2017. Anal. Chem. 89, 8731-8737.

Hsieh, K., Patterson, A. S., Ferguson, B. S., Plaxco, K. W., Soh, H. T., 2012. Angew. Chem. Int. Ed. 51, 4896-4900.

Huang, W. H., Pang, D. W., Tong, H., Wang, Z. L., Cheng, J. K., 2001. Anal. Chem. 73, 1048-1052.

Huang, Y. Z., Li, L., Zhang, Y., Zhang, L. N., Ge, S. G., Li, H., Yu J. H., 2017. ACS Appl. Mater. Interfaces 9, 32591-32598.

Kim, J., Lee, J. B., 2016. Nanoscale Res. Lett. 11:244.

Li, T., Wang, E. K., Dong, S. J., 2010. Anal. Chem. 82, 1515-1520.

Li, Y. J., Wang, C., Zhu, Y. B., Zhou, X. H., Xiang, Y., He, M., Zeng, S. Y., 2017. Biosens. Bioelectron. 89, 758-763.

Liang, W. B., Zhuo, Y., Zheng, Y. N., Xiong, C. Y., Chai, Y. Q., Yuan R., 2017. ACS Appl. Mater. Interfaces 9, 39812-39820.

Liu, M., Zhang, Q., Chang, D. R., Gu, J., Brennan, J. D., Li, Y. F., 2017b. Angew. Chem. Int. Ed. 56, 6142-6146.

Liu, W., Dong, H., Zhang, L. M., Tian, Y., 2017a. Angew. Chem. Int. Ed. 56, 16328-16332.

Liu, X. J., Song, M. M., Hou, T., Li, F., 2017c. ACS Sens. 2, 562-568.

Rudd, N. D., Wang, H., Fuentes-Fernandez, E. M. A., Teat, S. J., Chen, F., Hall, G., Chabal, Y. J., Li, J., 2016. ACS Appl. Mater. Interfaces 8, 30294-30303.

Sempionatto, J. R., Mishra, R. K., Martin, A., Tang, G. D., Nakagawa, T., Lu, X. L.,

Campbell, A. S., Lyu, K. M., Wang, J., 2017. ACS Sens. 2, 1531-1538.

Shi, Y., Wang, H. Y., Jiang, X. X., Sun, B., Song, B., Su, Y. Y., He, Y., 2016. Anal. Chem. 88, 3723-3729.

Shin, S. R., Kilic, T., Zhang, Y. S., Avci, H., Hu, N., Kim, D., Branco, C., Aleman, J., Massa, S., Silvestri, A., Kang, J., Desalvo, A., Hussaini, M. A., Chae, S. K., Polini, A., Bhise, N., Hussain, M. A., Lee, H., Dokmeci, M. R., Khademhosseini, A., 2017. Adv. Sci. 5, 1600522.

Sun, H., Li, W. B., Dong, Z. Z., Hu, C., Leung, C. H., Ma, D. L., Ren, K. N., 2018. Biosens. Bioelectron. 99, 361-367.

Tan, Y., Qiu, J. Z., Cui, M. Y., Wei, X. F., Zhao, M. M., Qiu, B., Chen, G. N., 2016. Analyst 141, 1121-1126.

Tang, S. R., Tong, P., Li, H., Tang, J., Zhang, L., 2013. Biosens. Bioelectron. 42, 608-611.

Tian, Y., Mao, L. Q., Okajima, T., Ohsaka, T., 2005. Biosens. Bioelectron. 21, 557-564.

Wang, F. L., Wu, Z., Lu, Y. X., Wang, J., Jiang, J. H., Yu, R. Q., 2010. Anal. Biochem. 405, 168-173.

Xu, H. Y., Zhou, S., Jiang, D. C., Chen, H. Y., 2018. Anal. Chem. 90, 1054-1058.

Yu, Y. J., Yu, C., Niu, Y. Z., Chen, J., Zhao, Y. L., Zhang, Y. C., Gao, R. F., He, J. L., 2018. Biosens. Bioelectron. 101, 297-303.

Zang, Y., Lei, J. P., Hao, Q., Ju, H. X., 2014. ACS Appl. Mater. Interfaces 6, 15991-15997.

Zhang, F. T., Nie, J., Zhang, D. W., Chen, J. T., Zhou, Y. L., Zhang, X. X., 2014. Anal. Chem. 86, 9489-9495.

Zhang, W., Xu, Y. W., Zou, X. B., Wang, P., 2017a. Biosens. Bioelectron. 97, 267-272.

Zhang, X. W., Qiu, Q. F., Jiang, H., Zhang, F. L., Liu, Y. L., Amatore, C., Huang, W. H., 2017b. Angew. Chem. Int. Ed. 56, 12997-13000.

Zhao, D. L., Siebold, D., Alvarez, N. T., Shanov, V. N., Heineman, W. R., 2017. Anal. Chem. 89, 9654-9663.

Zhao, X. H., Kong, R. M., Zhang, X. B., Meng, H. M., Liu, W. N., Tan, W. H., Shen, G. L., Yu, R. Q., 2011. Anal. Chem. 83, 5062-5066.

Zhao, Y. Y., Zhou, L., Tang, Z., 2013. Nat. Commun. 4:1493.

Zhou, Q., Lin, Y. X., Lin, Y. P., Wei, Q. H., Chen, G. N., Tang, D. P., 2016. Biosens. Bioelectron. 78, 236-243.

Zhu, Y. Y., Deng, D. Q., Xu, L. G., Zhu, Y. B., Wang, L. M., Qi, B., Xu, C. L., 2015. Anal. Methods 7, 662-666.

Zhuang, J. Y., Fu, L. B., Xu, M. D., Zhou, Q., Chen, G. N., Tang, D. P., 2013. Biosens. Bioelectron. 45, 52-57.

Figures caption

Scheme 1. Principle and procedures of the dual Pb^{2+}-DNAzyme feedback amplification strategy for Pb^{2+} sensing based on a micropipette tip-based miniaturized electrochemical device.

Figure 1. SEM images of (A) the interface of carbon fiber and wax, (B) the carbon fiber. Samples were prepared by coating a sputtered Au layer with a time interval 90 s. Microscope images of (C) the interface of carbon fiber and wax, (D) the joint of copper wire and carbon fiber.

Figure 2. Polyacrylamide gel characterization of the feedback system for Pb^{2+} sensing. Lane 1, DNA marker; lane 2, C1; lane 3, C2; lane 4, L-DNA; lane 5, the ligase product of C1 and L-DNA; lane 6, the ligase product of C2 and L-DNA; lane 7, the ligase product of C1, C2 and L-DNA; the reaction of the feedback amplification sensing system incubated with (lane 8) without (lane 9) Pb^{2+}. All the final concentration of the samples is 4 μM. (B) ACV responses of blank sample (a) and the sensing system were incubated without (b) and with (c) C2. (C) UV-Vis characterization of (a) the feedback amplification system and the sensing system were incubated without (b) and with (c) C2. Inset: the photograph shows the corresponding color change of the sample solution.

Figure 3. (A) ACV responses of the sensing system after incubating with different concentrations of Pb^{2+}: (a) 0 fM, (b) 0.2 pM, (c) 0.5 pM, (d) 1 pM, (e) 5 pM, (f) 10 pM, (g) 50 pM (h) 100 pM, (i) 500 pM, (j) 1 nM, (k) 10 nM (l) 100 nM. (B) ACV peak current plots versus the logarithm concentration of Pb^{2+}.

Figure 4. (A) The selectivity of the sensing system for 0.5 nM Pb^{2+} against various kinds of interference ions (Fe^{3+}, Mn^{2+}, Ag^{+}, Ba^{2+}, Cu^{2+}, Al^{3+}, Ca^{2+},

Ni^{2+}, Cd^{2+}, Co^{2+}, Cr^{3+} and Hg^{2+} each 50 nM). (B) Reproducibility of the sensing system with incubating 0.5 nM Pb^{2+}.

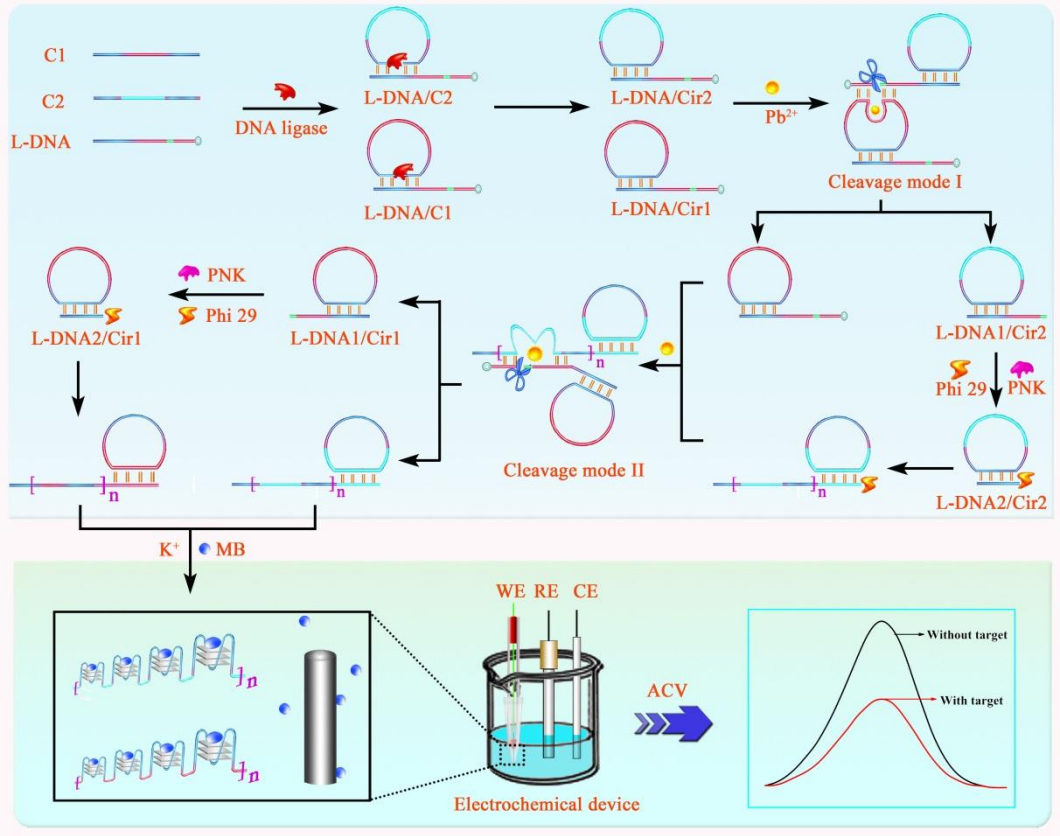

Scheme 1

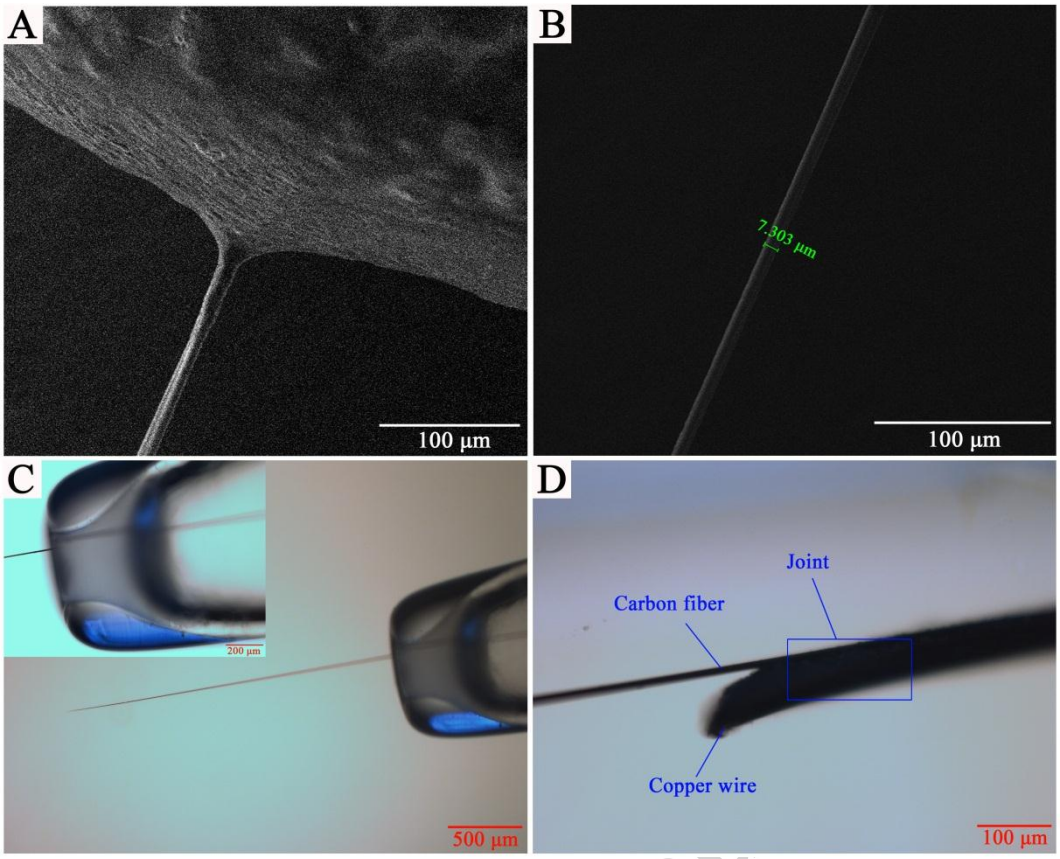

Figure 1

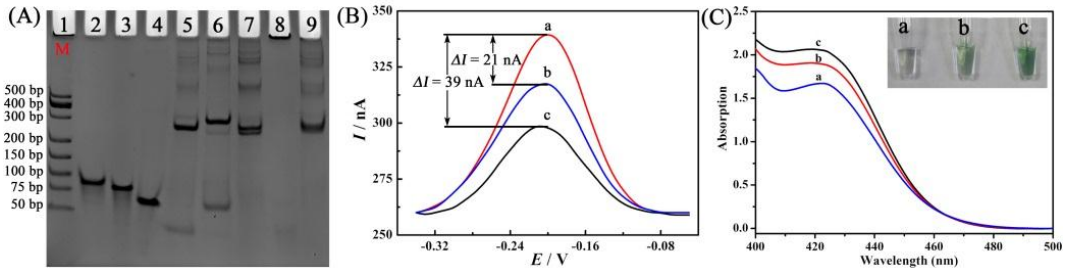

Figure 2

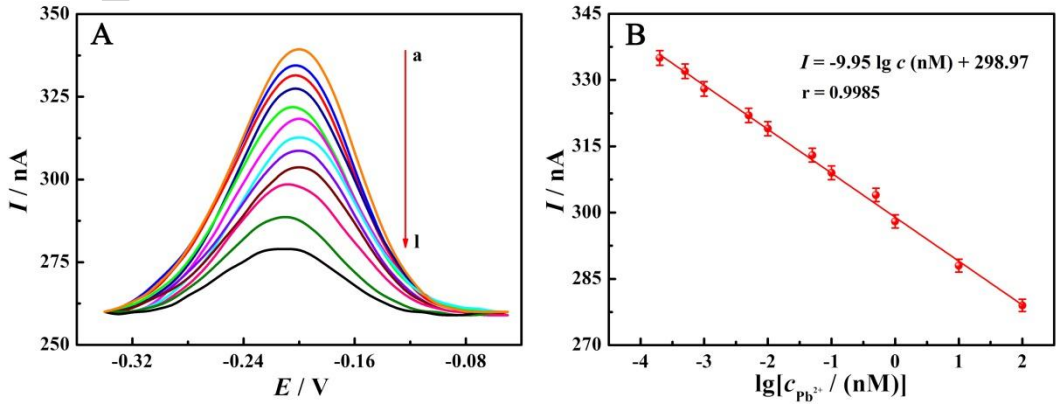

Figure 3

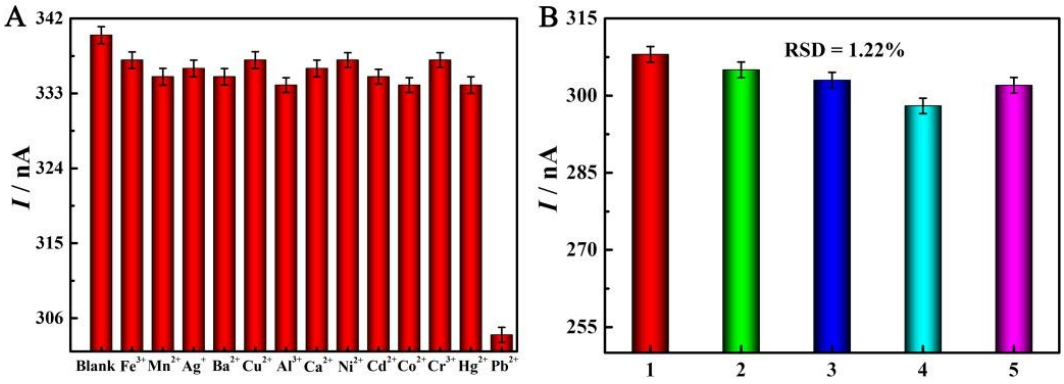

Figure 4

Table 1. Determination of Pb^{2+} in river samples by the proposed sensing system and AAS.

Samples	Found (M)	Recovery (%)	RSD (%) (n=3)	AAS Found (M)	Relative error (%)
Sample 1 (107° 4′ 1″ E, 29° 49′ 19″ N)	1.65×10^{-8}	106.7	3.7	1.54×10^{-8}	7.1
Sample 2 (107° 22′ 39″ E, 29° 43′ 6″ N)	1.72×10^{-8}	96.1	2.8	1.79×10^{-8}	-3.9
Sample 3 (107° 43′ 40″ E, 29° 52′ 29″ N)	2.54×10^{-8}	103.2	3.1	2.46×10^{-8}	3.3

Sample 4 (108° 43′ 36″ E, 30° 55′ 27″ N)	1.60 × 10^{-8}	94.7	3.4	1.69 × 10^{-8}	-5.3
Sample 5 (109° 52′ 46″ E, 31° 4′ 30″ N)	1.27 × 10^{-8}	97.7	3.5	1.30 × 10^{-8}	-2.3

Highlights

- Integrating dual Pb^{2+}-DNAzyme into one RCA-mediated feedback amplification for Pb^{2+} detection.
- Presenting a facile and efficient method for carbon fiber microelectrode fabrication.
- Reducing analyte sample volume down to microliter level.
- Analytical performance of the sensing system is down to picomole level.
- Displaying excellent applicability for evaluating Pb^{2+} in real samples.